# Electrochemical Behavior and Characterization of Semiquinone Radical Anion Species of Coenzyme PQQ in Aprotic Organic Media

**Shinobu Itoh,* Hirokatsu Kawakami, and Shunichi Fukuzumi***

*Contribution from the Department of Material and Life Science, Graduate School of Engineering, Osaka University, 2-1 Yamada-oka, Suita, Osaka 565-0871, Japan*

*Received April 21, 1998*

**Abstract:** Electrochemical behavior of coenzyme PQQ has been investigated in aprotic organic solvents using the trimethyl ester of PQQ ($\mathbf{1}_{ox}$H, trimethyl 4,5-dihydro-4,5-dioxo-1*H*-pyrrolo[2,3-*f*]quinoline-2,7,9-tricarboxylate) and its 1-methylated derivative ($\mathbf{1}_{ox}$Me, trimethyl 4,5-dihydro-4,5-dioxo-1-methylpyrrolo[2,3-*f*]-quinoline-2,7,9-tricarboxylate). $\mathbf{1}_{ox}$H shows a complicated cyclic voltammogram in organic media ($CH_2Cl_2$, MeCN, and DMSO); there are at least three reduction peaks and four oxidation peaks. The first irreversible reduction peak of $\mathbf{1}_{ox}$H around −0.9 V vs ferrocene/ferricenium ($Fc/Fc^+$) is very close to that of the reversible reduction peak of $\mathbf{1}_{ox}$Me. Addition of an equimolar amount of acetic acid into the solution of $\mathbf{1}_{ox}$Me results in a change of the reversible one-electron redox couple of $\mathbf{1}_{ox}$Me/$\mathbf{1}_{rad}$Me$^-$ to an irreversible one as observed in $\mathbf{1}_{ox}$H. This phenomenon indicates that protonation of the semiquinone radical anion causes disproportionation of the resulting neutral semiquinone $\mathbf{1}_{rad}H_2$ into (1/2) $\mathbf{1}_{ox}$H (quinone) and (1/2) $\mathbf{1}_{red}H_3$ (quinol). In this case, $\mathbf{1}_{ox}$H itself in bulk solution acts as the proton source to be converted into $\mathbf{1}_{ox}^-$. This is confirmed by the observation of reversible redox peaks due to a $\mathbf{1}_{ox}^-/\mathbf{1}_{rad}^{2-}$ couple at −1.30 vs $Fc/Fc^+$ in DMSO and by the 2:1 formation of $\mathbf{1}_{ox}^-$ and $\mathbf{1}_{red}H_3$ in the thin layer UV−vis spectrum of $\mathbf{1}_{ox}$H electrolyzed at −0.8 V $Ag/Ag^+$. Solution ESR spectra of electrochemically generated semiquinone radical anion species, $\mathbf{1}_{rad}H^-$, $\mathbf{1}_{rad}Me^-$, and $\mathbf{1}_{rad}^{2-}$, as well as the UV−vis spectrum of $\mathbf{1}_{rad}Me^-$ are also reported to explore the electronic structures of the semiquinone radical anion species of coenzyme PQQ. Addition of $Ca^{2+}$, which is another cofactor of quinoprotein alcohol dehydrogenases, into the solution of $\mathbf{1}_{ox}$Me causes ca. 0.57 V positive shift of the one-electron reduction potential of $\mathbf{1}_{ox}$Me, showing the enhancement of the oxidation power of $\mathbf{1}_{ox}$Me by a strong interaction between $Ca^{2+}$ and $\mathbf{1}_{rad}Me^-$. The ESR spectrum of $\mathbf{1}_{rad}Me^-$−$Ca^{2+}$ complex is successfully detected and compared with that of the free semiquinone radical anion $\mathbf{1}_{rad}Me^-$.

## Introduction

PQQ (pyrroloquinolinequinone) is a redox coenzyme that is involved in the catalysis of bacterial alcohol and glucose dehydrogenases and the subsequent electron transfer to the biological electron acceptors such as cytochrome *c* via ubiquinone.[1,2] In addition to the enzymological importance, the growth stimulating activity for microorganisms,[3] the pharmaceutical activities,[4] and the nutritional importance[5] of PQQ itself have been revealed to indicate that PQQ serves versatile functions in several living systems. Most of such biological functions have been attributed to the redox activity of coenzyme PQQ. This coenzyme has also been applied as an electrochemical mediator for the development of bioelectrochemical reactors and detectors and as a redox catalyst in some synthetic organic reactions.[6,7] In recent years, we have developed a series of PQQ model compounds and investigated their redox reactions with biologically important substances such as amines and alcohols in aprotic organic media, providing valuable information about the redox functions of coenzyme PQQ in vitro.[8−10]

* Corresponding author e-mail: itoh@chem.eng.osaka-u.ac.jp, fukuzumi@chem.eng.osaka-u.ac.jp. Tel: +81-6-879-7368. Fax: +81-6-879-7370.

(1) Anthony, C. In *Principles and Applications of Quinoproteins*; Davidson, V. L., Ed.; Marcel Dekker: New York, 1993; pp 17−45.

(2) Matsushita, K.; Adachi, O. In *Principles and Applications of Quinoproteins*; Davidson, V. L., Ed.; Marcel Dekker: New York, 1993; pp 47−71.

(3) (a) Ameyama, M.; Shinagawa, E.; Matsushita, K.; Adachi, O. *Agric. Biol. Chem*. **1984**, *48*, 2909. (b) Shimao, M.; Yamamoto, H.; Ninomiya, K.; Kato, N.; Adachi, O.; Ameyama, M.; Sakazawa, C. *Agric. Biol. Chem*. **1984**, *48*, 2873. (c) Ameyama, M.; Shinagawa, E.; Matsushita, K.; Adachi, O. *Agric. Biol. Chem*. **1984**, *48*, 3099. (d) Ameyama, M.; Shinagawa, E.; Matsushita, K.; Adachi, O. *Agric. Biol. Chem*. **1985**, *49*, 699. (e) Ameyama, M.; Matsushita, K.; Shinagawa, E.; Hayashi, M.; Adachi, O. *BioFactors* **1988**, *1*, 51. (f) Adachi, O.; Okamoto, K.; Matsushita, K.; Shinagawa, E.; Ameyama, M. *Agric. Biol. Chem*. **1990**, *54*, 2751.

(4) (a) Watanabe, A.; Hobara, N.; Tsuji, T. *Curr. Ther. Res.* **1988**, *44*, 896. (b) Watanabe, A.; Hobara, N.; Ohsawa, T.; Higashi, T.; Tsuji, T. *Hiroshima J. Med. Sci*. **1989**, *38*, 49. (c) Nishigori, H.; Yasunaga, M.; Mizumura, M.; Lee, J. W.; Iwatsuru, M. *Life Sci.* **1989**, *45*, 593. (d) Hamagishi, Y.; Murata, S.; Kamei, H.; Oki, T.; Adachi, O.; Ameyama, M. *J. Pharmacol. Exp. Ther*. **1990**, *255*, 980.

(5) (a) Killgore, J.; Smidt, C.; Duich, L.; Romero-Chapman, N.; Tinker, D.; Reiser, K.; Melko, M.; Hyde. D.; Rucker, R. B. *Science* **1989**, *245*, 850. (b) Smidt, C. R.; Steinberg, F. M.; Rucker, R. B. *Proc. Soc. Exp. Biol. Med.* **1991**, *197*, 19.

(6) (a) Lion-Dagan, M.; Katz, E.; Willner, I. *J. Am. Chem. Soc*. **1994**, *116*, 7913. (b) Katz, E.; Lötzbeyer, T.; Schlereth, D. D.; Schuhmann, W.; Schmidt, H.-L. *J. Electroanal. Chem*. **1994**, *373*, 189. (c) Katz, E.; Lion-Dagan, M.; Willner, I. *J. Electroanal. Chem*. **1995**, *382*, 25. (d) Bardea, A.; Katz, E.; Bückmann, A. F.; Willner, I. *J. Am. Chem. Soc*. **1997**, *119*, 9114. (e) Esaka, Y.; Kano, K.; Sukeguchi, M.; Goto, M. *Anal. Sci.* **1993**, *9*, 207. (f) Kuwabata, S.; Tsuda, R.; Yoneyama, H. *J. Am. Chem. Soc.* **1994**, *116*, 5437.

(7) (a) Hirao, T.; Murakami, T.; Ohno, M.; Ohshiro, Y. *Chem. Lett.* **1989**, 785. (b) Hirao, T.; Ohno, M.; Ohshiro, Y. *Tetrahedron Lett.* **1990**, *31*, 6039. (c) Hirao, T.; Murakami, T.; Ohno, M.; Ohshiro, Y. *Chem. Lett*. **1991**, 299.

(8) (a) Itoh, S.; Mure, M.; Ogino, M.; Ohshiro, Y. *J. Org. Chem*. **1991**, *56*, 6857. (b) Itoh, S.; Mure, M.; Suzuki, A.; Murao, H.; Ohshiro, Y. *J. Chem. Soc., Perkin Trans. 2* **1992**, 1245.

S0002-7863(98)01366-3 CCC: $15.00 
Published on Web 07/11/1998

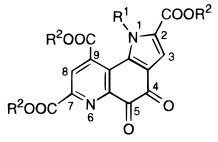

PQQ: $R^1 = R^2 = H$
$\mathbf{1}_{ox}$H: $R^1 = H$, $R^2 = Me$
$\mathbf{1}_{ox}$Me: $R^1 = R^2 = Me$

Coenzyme PQQ shows a reversible cyclic voltammogram in aqueous media, which corresponds to the two-electron redox reaction between the quinone and the quinol: $E_{1/2} = -175$ mV vs SCE (66 mV vs NHE) at pH 7.0.[11a,12] Kano and co-workers analyzed the reversible voltammogram using a digital simulation program to evaluate the standard redox potentials for the quinone/semiquinone and semiquinone/quinol couples as well as the acid−base dissociation constants of the quinone, semiquinone, and quinol.[11b] On the other hand, Bruice and co-workers demonstrated that the electrochemistry of the trimethyl ester of coenzyme PQQ ($\mathbf{1}_{ox}$H) in aprotic organic solvents involving irreversible redox waves is not as simple as that of PQQ in aqueous media.[13] The complicated redox behavior of coenzyme PQQ in aprotic organic media seems to require the scrutiny of the assignment of each redox wave. Moreover, the semiquinone radical anion species of PQQ derivatives in nonaqueous media have not yet been fully characterized. Lack of information about the redox property of coenzyme PQQ in nonaqueous media has precluded our deeper understanding of the electron transfer mechanism of the quinoproteins, since PQQ is buried inside the protein matrix in a hydrophobic environment, allowing only limited access to protons.[14,15]

On the other hand, the crystal structure of quinoprotein methanol dehydrogenase (MDH) from methylotrophic bacteria has been recently determined by two independent research groups to provide full particulars of the enzyme active center.[14,15] According to the reported X-ray structure, there is one calcium ion strongly bound to PQQ through its C-5 quinone carbonyl oxygen, N-6 pyridine nitrogen, and C-7 carboxylate group in the enzyme active site. We have recently shown that $\mathbf{1}_{ox}$H and its derivatives strongly bind to $Ca^{2+}$ at the same position as that observed in the enzymatic system.[10b,c]

We report herein the scrutiny of electrochemistry of $\mathbf{1}_{ox}$H and its derivatives in aprotic organic media as well as the full characterization of the electrochemically generated semiquinone radical anion species by ESR and UV−vis spectroscopies. In addition, interaction between the radical anion species and $Ca^{2+}$, which is another cofactor of quinoprotein alcohol dehydrogenases,[14,15] has been successfully explored by means of cyclic voltammetry and ESR techniques. These data provide valuable insight into the versatile redox functions of coenzyme PQQ in both the enzymatic and the nonenzymatic systems.

## Experimental Section

The trimethyl ester of coenzyme PQQ ($\mathbf{1}_{ox}$H) was obtained from the previous studies.[8−10] The other chemicals used in this study except compounds $\mathbf{1}_{ox}$H, $\mathbf{1}_{ox}$Me, **2**, and **3** were commercial products of the highest available purity and were further purified by the standard methods, if necessary.[16] Melting points were determined on a Yamato MP-21 apparatus and were uncorrected. IR spectra were recorded with a Shimadzu FTIR-8200PC. Mass spectra were recorded with a Jeol JNX-DX303 HF mass spectrometer. $^1$H and $^{13}$C NMR spectra were recorded on a Jeol FT-NMR EX-270 spectrometer.

The cyclic voltammetric measurements were performed on a BAS 100B electrochemical analyzer in anhydrous $CH_2Cl_2$, MeCN, or DMSO containing 0.10 M $NBu_4PF_6$ as supporting electrolyte. The organic solvents were dried over $CaH_2$ and distilled at least three times just before use for the experiments. The Au working electrodes (BAS) were polished with BAS polishing alumina suspension and rinsed with acetone before use. The counter electrode was a platinum wire. A silver pseudo-reference electrode was used, and the potentials are referenced versus the ferrocene/ferricenium couple. All electrochemical measurements were carried out at 25 °C under an atmospheric pressure of nitrogen.

Thin-layer UV−visible spectrum of the electrochemically generated radical anion $\mathbf{1}_{rad}Me^-$ was taken by using a 0.5 mm path length quartz cell connected to the bottom of a three-necked vessel (ca. 20 mL capacity). An optically transparent platinum thin-layer electrode, which was placed in the quartz cell, was used as the working electrode and silver wires were used as counter and reference electrodes. Bulk electrolysis of $\mathbf{1}_{ox}$Me ($5.4 \times 10^{-4}$ M) was carried out at −0.80 V vs $Ag/Ag^+$ in anhydrous $CH_2Cl_2$ containing 0.1 M $NBu_4PF_6$ at 25 °C. UV−visible spectrum was recorded on a Hewlett-Packard 8453 photodiode array spectrophotometer.

ESR spectra of electrochemically generated semiquinone radical anion species of the quinones were taken on a Jeol JES-ME-2X by using an electrolysis cell designed for ESR measurements.[17] The ESR cell is composed of a helical gold wire with large surface area (12 $cm^2$) as the working electrode, which can generate enough semiquinone radical anions to detect the ESR spectra, and silver wires as counter and reference electrodes. The controlled potential electrolysis of the quinone was carried out in anhydrous $CH_2Cl_2$ or MeCN containing 0.10 M $NBu_4PF_6$ as supporting electrolyte in the ESR cavity. The $g$ values were determined using a $Mn^{2+}$ marker as a reference. Computer simulation of the ESR spectra were carried out by using ESRaII Version 1.01 (Calleo Scientific Publisher) on a Macintosh personal computer.

The theoretical studies were performed using the PM3 method. The calculations were performed by using a MOL-MOLIS program Version 2.8 (Daikin Industries, Ltd) or a Spartan program (Version 5.0, Wavefunction, Inc.). Final geometries and energetics were obtained by optimizing the total molecular energy with respect to all structural variables. The geometries of the radicals were optimized using the unrestricted Hartree−Fock (UHF) formalism.

**Synthesis of $\mathbf{1}_{ox}$Me.[18]** A mixture of **2** (trimethyl 5-methoxypyrrolo-[2,3-*f*]quinoline-2,7,9-tricarboxylate, 11.7 mg, 0.031 mmol),[19] $K_2CO_3$ (284 mg, 2.0 mmol), and MeI (1.3 mL, 20 mmol) in anhydrous DMF (3.0 mL) was stirred at room temperature for 24 h. Removal of the solvent and MeI under reduced pressure at 80 °C gave an orange color material that was dissolved into ether and washed with water several

(9) (a) Itoh, S.; Kato, J.; Inoue, T.; Kitamura, Y.; Komatsu, M.; Ohshiro, Y. *Synthesis* **1987**, 1067−1071. (b) Itoh, S.; Fukui, Y.; Ogino, M.; Haranou, S.; Komatsu, M.; Ohshiro, Y. *J. Org. Chem.* **1992**, *57*, 2788. (c) Itoh, S.; Fukui, Y.; Haranou, S.; Ogino, M.; Komatsu, M.; Ohshiro, Y. *J. Org. Chem.* **1992**, *57*, 4452.

(10) (a) Itoh, S.; Ogino, M.; Fukui, Y.; Murao, H.; Komatsu, M.; Ohshiro, Y.; Inoue, T.; Kai, Y.; Kasai, N. *J. Am. Chem. Soc.* **1993**, *115*, 9960. (b) Itoh, S.; Kawakami, H.; Fukuzumi, S. *J. Am. Chem. Soc.* **1997**, *119*, 439. (c) Itoh, S.; Kawakami, H.; Fukuzumi, S. *Biochemistry* **1998**, *37*, 6562.

(11) (a) Kano, K.; Mori, K.; Uno, B.; Kubota, T.; Ikeda, T.; Senda, M. *Bioelectrochem. Bioenerg.* **1990**, *24*, 193. (b) Kano, K.; Mori, K.; Uno, B.; Kubota, T.; Ikeda, T.; Senda, M. *Bioelectrochem. Bioenerg.* **1990**, *23*, 227.

(12) Duine et al. determined the redox potential of the quinone/quinol couple as 90 mV vs NHE at pH 7.0 by a potentiometric titration: Duine, J. A.; Frank, J.; Verwiel, P. E. J. *Eur. J. Biochem.* **1981**, *118*, 395.

(13) Eckert, T. S.; Bruice, T. C.; Gainor, J. A.; Weinreb, S. M. *Proc. Natl. Acad. Sci. U.S.A.* **1982**, *79*, 2533.

(14) (a) White, S.; Boyd, G.; Mathews, F. S.; Xia, Z.-x.; Dai, W.-w.; Zhang, Y.-f.; Davidson, V. L. *Biochemistry* **1993**, *32*, 12955. (b) Xia, Z.-x.; Dai, W.-w.; Zhang, Y.-f.; White, S. A.; Boyd, G. D.; Mathews, F. S. *J. Mol. Biol.* **1996**, *259*, 480.

(15) (a) Blake, C. C. F.; Ghosh, M.; Harlos, K.; Avezoux, A.; Anthony, C. *Nat. Struct. Biol.* **1994**, *1*, 102. (b) Cozier, G. E.; Giles, I. G.; Anthony, C. *Biochem. J.* **1995**, *308*, 375. (c) Ghosh, M.; Anthony, C.; Harlos, K.; Goodwin, M. G.; Blake, C. *Structure* **1995**, *3*, 177.

(16) Perrin, D. D.; Armarego, W. L. F.; Perrin, D. R. *Purification of Laboratory Chemicals*; Pergamon Press: Elmsford, NY, 1966.

(17) Ohya-Hishiguchi, H. *Bull. Chem. Soc. Jpn.* **1979**, *52*, 2064.

(18) Although we have already reported the synthetic procedure of $\mathbf{1}_{ox}$-Me,[9a] an easier way for the preparation of the synthetic intermediate **3** has been developed in this study.

(19) The starting material **2** was synthesized by the reported procedures; Corey, E. J.; Tramontano, A. *J. Am. Chem. Soc.* **1981**, *103*, 5599.

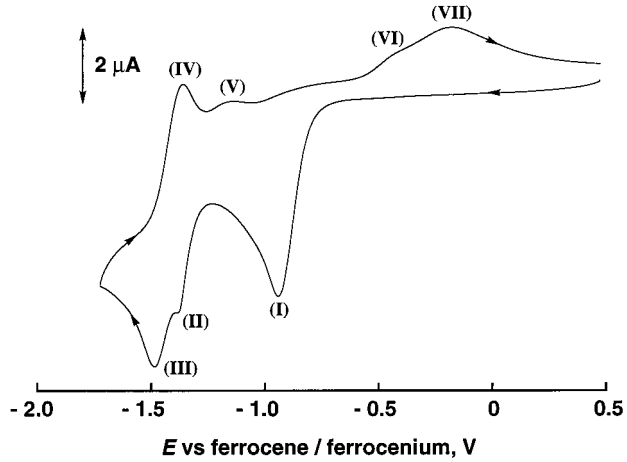


**Figure 1.** Cyclic voltammogram of $\mathbf{1}_{ox}$H ($1.5 \times 10^{-3}$ M) in deaerated $CH_2Cl_2$ containing 0.10 M $Bu_4NPF_6$ with an Au electrode at 298 K; sweep rate 100 mV $s^{-1}$.

times to remove the inorganic materials. After treatment of the organic layer with $MgSO_4$, evaporation of the solvent gave an orange solid **3** (trimethyl 1-methyl-5-methoxypyrrolo[2,3-*f*]quinoline-2,7,9-tricarboxylate) quantitatively. The $^1$H and $^{13}$C NMR spectra, the IR spectrum, and the melting point of the product were identical to those of the authentic sample of **3**.[9a] Compound **3** was converted into $\mathbf{1}_{ox}$Me by the oxidation with CAN (ceric ammonium nitrate) according to the reported procedure.[9a]

**Preparation of Potassium Salt of $\mathbf{1}_{ox}^-$.** Addition of 2 equiv of KCN dissolved in water to an MeCN solution of $\mathbf{1}_{ox}$H (5 mM) resulted in immediate precipitation of dark green solids that were isolated by centrifugation and washed with MeCN several times: 100% yield; mp 265−270 °C (dec); IR (KBr) 1726 (ester C═O), 1644 (quinone), 1478 (C═C), 1230, 1210 $cm^{-1}$ (C−O); $^1$H NMR (DMSO-$d_6$) $\delta$ 3.68 (3 H, s, −$COOCH_3$), 3.89 (3 H, s, −$COOCH_3$), 3.92 (3 H, s, −$COOCH_3$), 6.98 (1 H, s, $H_3$), 7.93 (1 H, s, $H_8$); $^{13}$C NMR (DMSO-$d_6$) 50.4, 52.4, 52.8 (−$OCH_3$), 101.2, 124.7, 125.3, 132.7, 136.6, 139.4, 143.1, 143.6, 146.1 (9 aromatic carbons), 164.2, 164.3, 167.7 (3 ester C═O), 171.5, 183.0 (2 quinone C═O) ppm; MS (FAB) *m*/*z* 412 ($M^+ + 2$, characteristic peak for *o*-quinone compounds), 374 ($M^+ + 2 - K^+$); UV−vis (MeCN) $\lambda_{max} = 360$ nm ($\epsilon = 22\,600$ $M^{-1}$ $cm^{-1}$). Anal. Calcd for $C_{17}H_{11}N_2O_8K$: C, 49.76; H, 2.70; N, 6.83. Found: C, 49.95; H, 2.83; N, 7.10.

When KOH was used instead of KCN, the partial hydrolysis of the ester groups of $\mathbf{1}_{ox}$H occurred to decrease the yield of $\mathbf{1}_{ox}^-$ slightly (90%).

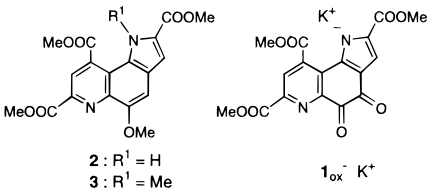


## Results and Discussion

**Electrochemistry.** Figure 1 shows a cyclic voltammogram of $\mathbf{1}_{ox}$H in $CH_2Cl_2$, which gives irreversible reduction (cathodic) peaks at −0.94 V (peak I) and −1.38 V (peak II) and irreversible oxidation (anodic) peaks at −1.14 V (peak V), −0.43 V (peak VI), and −0.18 V (peak VII) with a reversible redox couple at $E_{1/2} = -1.42$ V vs ferrocene/ferricenium ($Fc/Fc^+$) (peaks III and IV). Similar voltammograms were obtained in MeCN and DMSO. However, the reduction and oxidation peak potentials except peaks VI and VII are shifted toward a positive direction in MeCN and DMSO as compared to those in $CH_2Cl_2$ (Table 1) due to the stronger solvation of MeCN and DMSO as discussed later.

**Table 1.** Reduction and Oxidation Peak Potentials of $\mathbf{1}_{ox}$H in Anhydrous Organic Solvents[a]

| | reduction peak potential | | | oxidation peak potential | | | |
|---|---|---|---|---|---|---|---|
| solvent | I | II | III | IV | V | VI | VII |
| $CH_2Cl_2$[b] | −0.94 | −1.38 | −1.48 | −1.36 | −1.14[d] | −0.43[d] | −0.18 |
| MeCN[b] | −0.75 | −1.25 | −1.39 | −1.29 | −1.06[d] | −0.18 | |
| DMSO[c] | −0.80 | −1.23 | −1.34 | −1.25 | −1.07 | −0.61 | −0.20[d] |

[a] V vs ferrocene/ferricenium ($Fc/Fc^+$). [b] Sweep rate = 100 mV $s^{-1}$. [c] Sweep rate = 20 mV $s^{-1}$. [d] Very small.

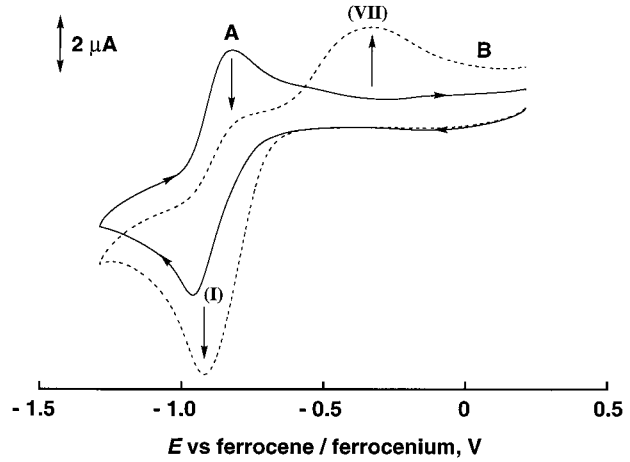


**Figure 2.** Cyclic voltammograms of $\mathbf{1}_{ox}$Me ($1.4 \times 10^{-3}$ M) (A) in the absence of AcOH and (B) in the presence of AcOH ($1.4 \times 10^{-3}$ M) in deaerated $CH_2Cl_2$ containing 0.10 M $Bu_4NPF_6$ with an Au electrode at 298 K; sweep rate 100 mV $s^{-1}$.

When the pyrrole proton of $\mathbf{1}_{ox}$H is replaced by a methyl group to give $\mathbf{1}_{ox}$Me, the cyclic voltammogram of $\mathbf{1}_{ox}$Me in $CH_2Cl_2$ exhibits a clearly reversible redox couple at $E_{1/2} = -0.90$ V vs $Fc/Fc^+$, which corresponds to the one-electron redox couple of $\mathbf{1}_{ox}$Me/$\mathbf{1}_{rad}$Me$^-$ as shown in Figure 2A.[20] The reduction peak potential of this couple (−0.96 V) is very close to the reduction peak (I) of $\mathbf{1}_{ox}$H in $CH_2Cl_2$ shown in Figure 1. Upon addition of an equimolar amount of acetic acid into a $CH_2Cl_2$ solution of $\mathbf{1}_{ox}$Me, the reversible one-electron redox couple of $\mathbf{1}_{ox}$Me/$\mathbf{1}_{rad}$Me$^-$ becomes irreversible as shown in Figure 2B, where the oxidation peak current at −0.84 V disappears accompanied by the appearance of a new broad oxidation peak at −0.34 V. In the presence of acetic acid, electrochemically generated $\mathbf{1}_{rad}$Me$^-$ accepts a proton from the acid to give $\mathbf{1}_{rad}$MeH (neutral semiquinone radical). $\mathbf{1}_{rad}$MeH then spontaneously disproportionates into (1/2) $\mathbf{1}_{ox}$Me and (1/2) $\mathbf{1}_{red}$$MeH_2$ (quinol form), the latter of which is oxidized at the oxidation peak potential (−0.34 V). The integrals of wave I in Figure 2 of $\mathbf{1}_{ox}$Me alone (A) and $\mathbf{1}_{ox}$Me plus 1 equiv of acetic acid (B) show about 2-fold increase in the charge consumed during the reductive sweep. This is indicative of the transition from a one-electron to a two-electron reduction:

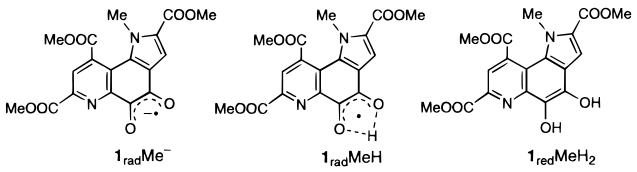


Since the cyclic voltammogram of $\mathbf{1}_{ox}$Me in the presence of acetic acid (Figure 2B) is very close to that of $\mathbf{1}_{ox}$H measured

(20) Further negative sweep provided an irreversible reduction peak of $\mathbf{1}_{rad}$Me$^-$ at −1.58 V vs $Fc/Fc^+$ in $CH_2Cl_2$.

within a similar potential range (+0.5 V to −1.3 V vs $Fc/Fc^+$, cf. Supporting Information, Figure S1), the reduction peak I can be assigned to the one-electron reduction of $\mathbf{1}_{ox}H$ to $\mathbf{1}_{rad}H^-$ (eq 1). In the case of $\mathbf{1}_{ox}H$, however, no coupled oxidation peak for $\mathbf{1}_{rad}H^-$ to $\mathbf{1}_{ox}H$ is observed, but instead a broad oxidation peak VII appears at −0.18 V. This can be attributed to intermolecular proton transfer from $\mathbf{1}_{ox}H$ in bulk solution to electrochemically generated semiquinone radical anion $\mathbf{1}_{rad}H^-$ in the electrochemical double layer.[21] Such a proton transfer from $\mathbf{1}_{ox}H$ to $\mathbf{1}_{rad}H^-$ generates $\mathbf{1}_{ox}^-$ and the neutral semiquinone $\mathbf{1}_{rad}H_2$ (eq 4). The generated $\mathbf{1}_{rad}H_2$ may easily disproportionate into (1/2) $\mathbf{1}_{ox}H$ and (1/2) $\mathbf{1}_{red}H_3$ (quinol form) as indicated in eq 6. Thus, the oxidation peak VII may correspond to the oxidation of $\mathbf{1}_{red}H_3$ to $\mathbf{1}_{rad}H_3^+$ (eq 10),[22] the latter of which spontaneously releases $H^+$ and continues the same reaction sequences (eqs 6 and 10) until all the reduced species are consumed.

Occurrence of the disproportionation reaction (eq 6) in the electrochemical reduction of $\mathbf{1}_{ox}H$ is confirmed by the spectrum obtained by bulk electrolysis of $\mathbf{1}_{ox}H$, which is almost identical to the calculated spectrum by assuming a mixture of $\mathbf{1}_{ox}^-$ and $\mathbf{1}_{red}H_3$ in a 2:1 ratio (see, Supporting Information, Figure S2).[23] This ratio agrees with the stoichiometry of the net reaction, since the acid−base equilibrium between $\mathbf{1}_{rad}H^-$ and $\mathbf{1}_{ox}H$ produces $\mathbf{1}_{rad}H_2$ and $\mathbf{1}_{ox}^-$ (eq 4) and the disproportionation of $\mathbf{1}_{rad}H_2$ results in (1/2) $\mathbf{1}_{ox}H$ and (1/2) $\mathbf{1}_{red}H_3$ (eq 6), so that one $\mathbf{1}_{rad}H^-$ produces $\mathbf{1}_{ox}^-$ and $\mathbf{1}_{red}H_3$ in 2:1 ratio.

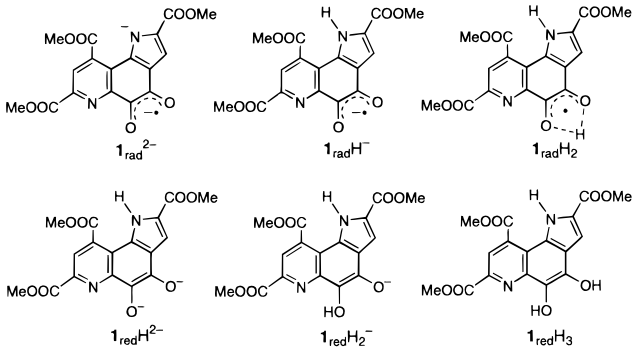


reduction

$$\mathbf{1}_{ox}H + e^- \longrightarrow \mathbf{1}_{rad}H^- \quad (1)$$

$$\mathbf{1}_{rad}H^- + e^- \longrightarrow \mathbf{1}_{red}H^{2-} \quad (2)$$

$$\mathbf{1}_{ox}^- + e^- \longrightarrow \mathbf{1}_{rad}^{2-} \quad (3)$$

acid-base equilibrium

$$\mathbf{1}_{rad}H^- + \mathbf{1}_{ox}H \rightleftharpoons \mathbf{1}_{rad}H_2 + \mathbf{1}_{ox}^- \quad (4)$$

$$\mathbf{1}_{red}H^{2-} + \mathbf{1}_{ox}H \rightleftharpoons \mathbf{1}_{red}H_2^- + \mathbf{1}_{ox}^- \quad (5)$$

disproportionation

$$\mathbf{1}_{rad}H_2 \longrightarrow 1/2\ \mathbf{1}_{ox}H + 1/2\ \mathbf{1}_{red}H_3 \quad (6)$$

oxidation

$$\mathbf{1}_{rad}^{2-} \longrightarrow \mathbf{1}_{ox}^- + e^- \quad (7)$$

$$\mathbf{1}_{red}H^{2-} \longrightarrow \mathbf{1}_{rad}H^- + e^- \quad (8)$$

$$\mathbf{1}_{red}H_2^- \longrightarrow \mathbf{1}_{rad}H_2 + e^- \quad (9)$$

$$\mathbf{1}_{red}H_3 \longrightarrow \mathbf{1}_{rad}H_3^+ + e^- \quad (10)$$

As mentioned above, $\mathbf{1}_{ox}H$ gives another reduction peak II at −1.38 V and a reversible redox couple at $E_{1/2} = -1.42$ V in $CH_2Cl_2$. We attributed the irreversible reduction peak at −1.38 V to the reduction of $\mathbf{1}_{rad}H^-$ to $\mathbf{1}_{red}H^{2-}$ (eq 2) and the reversible redox couple at −1.42 V to the redox reaction between $\mathbf{1}_{ox}^-$ and $\mathbf{1}_{rad}^{2-}$ (eqs 3 and 7), the former of which is generated from $\mathbf{1}_{ox}H$ by deprotonation (eq 4). To confirm the assignment of the reversible redox couple at −1.42 V in $CH_2Cl_2$, we have prepared a potassium salt of $\mathbf{1}_{ox}^-$ (see Experimental Section). Since $\mathbf{1}_{ox}^-K^+$ is sparingly soluble in $CH_2Cl_2$ and in MeCN but readily soluble in DMSO, the cyclic voltammogram of $\mathbf{1}_{ox}^-K^+$ in DMSO is compared with that of $\mathbf{1}_{ox}H$ in the same solvent. Figure 3B shows the cyclic voltammogram of $\mathbf{1}_{ox}H$ in DMSO. The electrochemical behavior of $\mathbf{1}_{ox}H$ in DMSO is essentially the same as in $CH_2Cl_2$. The isolated $\mathbf{1}_{ox}^-K^+$ gave a reversible redox couple at −1.30 V vs $Fc/Fc^+$ in DMSO (Figure 3A), which is superimposable to that of the reversible couple of $\mathbf{1}_{ox}H$ at −1.30 V vs $Fc/Fc^+$ (III and IV) in the same solvent system. Thus, it is confirmed that the reversible couple observed at the most negative region corresponds to the redox reaction between $\mathbf{1}_{ox}^-$ and $\mathbf{1}_{rad}^{2-}$ (eqs 3 and 7). Then, the oxidation peaks V and VI could be attributed to the oxidations of $\mathbf{1}_{red}H^{2-}$ (eq 8) and $\mathbf{1}_{red}H_2^-$ (eq 9), respectively. In fact, the oxidation peak VI does not appear when the cathodic sweep is returned at −1.15 V vs $Fc/Fc^+$ just before the reduction of $\mathbf{1}_{rad}H^-$; wave II (see Figure 2B and Supporting Information, Figure S1).

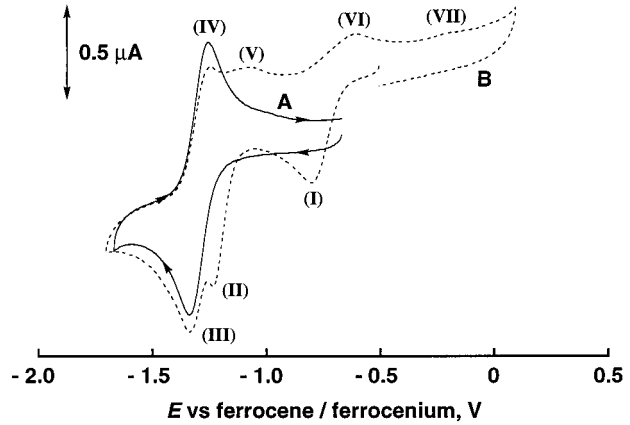


**Figure 3.** Cyclic voltammograms of (A) $\mathbf{1}_{ox}^-K^+$ ($1.4 \times 10^{-3}$ M) and (B) $\mathbf{1}_{ox}H$ ($1.7 \times 10^{-3}$ M) in deaerated DMSO containing 0.10 M $Bu_4NPF_6$ with an Au electrode at 298 K; sweep rate 20 mV $s^{-1}$.

During the course of our research, Rotello and co-workers reported a similar mechanism of the electrochemistry of flavin cofactor models in aprotic organic media, although they only discussed the first one-electron reduction.[24] It becomes clear that the electrochemical behavior of coenzyme PQQ in aprotic organic media is quite similar to that of flavin coenzyme, but PQQ possesses ca. 0.4 V higher oxidizing ability than flavin

(21) The p$K_a$ value of the pyrrole proton of $\mathbf{1}_{ox}H$ has been determined to be almost the same as that of $HN(C_2H_5)_3^+$.[8a]

(22) Although the exact reason for the difference in the oxidation peak potential (VII) between $\mathbf{1}_{red}H_3$ (−0.18 V) and $\mathbf{1}_{red}MeH_2$ (−0.34 V) is not clear at the present, the steric crowdedness due to the 1-methyl group in $\mathbf{1}_{red}MeH_2$ may induce some strain into the flat molecule of the fully reduced PQQ, and this strain may cause the negative shift of the oxidation potential of $\mathbf{1}_{red}MeH_2$ as compared to that of $\mathbf{1}_{red}H_3$. Theoretical calculations using the PM3 method suggest that the quinone and the semiquinone forms of PQQ can be distorted from the plane to some extent but the quinol form of PQQ should be plane. Thus, the oxidation of the quinol form would reduce the strain induced by the methyl group in $\mathbf{1}_{red}MeH_2$.

(23) The UV−vis spectra of $\mathbf{1}_{ox}^-$ and $\mathbf{1}_{red}H_3$ were taken independently by adding excess amounts of $Et_3N$ and $MeNHNH_2$ to a $CH_2Cl_2$ solution of $\mathbf{1}_{ox}H$, respectively; Itoh, S.; Ohshiro, Y.; Agawa, T. *Bull. Chem. Soc. Jpn.* **1986**, *59*, 1911.

(24) Niemz, A.; Imbriglio, J.; Rotello, V. M. *J. Am. Chem. Soc.* **1997**, *119*, 887.

**Table 2.** *g* Values and Hyperfine Splitting (hfs) Values (G) of the Semiquinone Radical Anion Species of Coenzyme PQQ Derivatives in Aprotic Organic Solvents[a]

| radical | solvent | *g* | $a_{H(1)}$ | $a_{H(3)}$ | $a_{H(8)}$ | $a_{N(1)}$ | $a_{N(6)}$ | $a_{Me(1)}$ | $a_{Me(e)}$[b] |
|---|---|---|---|---|---|---|---|---|---|
| $\mathbf{1}_{rad}Me^-$ | $CH_2Cl_2$ | 2.0034 | | 4.83 | 3.80 | 4.52 | 0.57 | 0.72 | 0.72 |
| $\mathbf{1}_{rad}H^-$ | $CH_2Cl_2$ | 2.0041 | 1.40 | 5.43 | 1.40 | 5.11 | 0.70 | | 0.70 |
| $\mathbf{1}_{rad}^{2-}$ | MeCN | 2.0039 | | 0.87 | 3.51 | 0.90 | 0.70 | | |
| $\mathbf{1}_{rad}Me^-$ | MeCN | 2.0038 | | 2.20 | 0.95 | 0.84 | 0.38 | 0.84 | |
| $\mathbf{1}_{rad}Me^-$ [c] | MeCN | 2.0044 | | 1.50 | 1.21 | 1.01 | 1.01 | 0.91 | |

[a] The hfs values determined by computer simulation (SIM in Figure 5) are assigned for each nucleus based on the calculated atomic orbital spin populations of the semiquinone radical anions (Supporting Information, Figures S3−S5). [b] For methyl ester group. [c] In the presence of $Ca(ClO_4)_2$ (1.0 mM, 1 equiv).

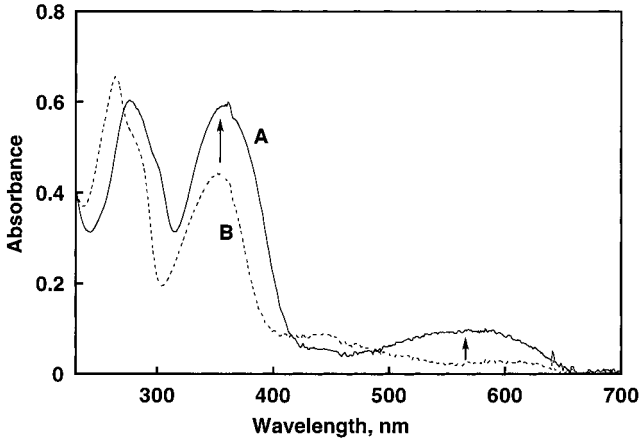


**Figure 4.** Thin-layer UV−vis spectra of (A) $\mathbf{1}_{rad}Me^-$ ($5.4 \times 10^{-4}$ M) electrochemically generated at − 0.8 V vs $Ag/Ag^+$ and (B) $\mathbf{1}_{ox}Me$ in deaerated $CH_2Cl_2$ at 298 K.

cofactor ($\mathbf{1}_{ox}Me/\mathbf{1}_{rad}Me^-$ couple: −0.9 V vs $Fc/Fc^+$; flavin/flavin semiquinone radical anion couple: −1.3 V vs $Fc/Fc^+$ [24]).

**Characterization of Radical Anion Species.** Figure 4A shows the UV−vis spectrum of $\mathbf{1}_{rad}Me^-$ generated by bulk electrolysis of $\mathbf{1}_{ox}Me$ at −0.8 V vs $Ag/Ag^+$ in $CH_2Cl_2$ containing 0.1 M $NBu_4PF_6$. It has strong absorptions at 276 and 360 nm together with a broad band at 570 nm. This spectrum is relatively similar to those of a monomeric phenanthrene semiquinone radical anion ($PQ_{rad}^-$) ($\lambda_{max}$ = 331 and 499 nm)[25] and a monomeric semiquinone radical anion of 9-decarboxy-PQQ (9-decarboxy-$PQQ_{rad}^-$) ($\lambda_{max}$ = 395 and ∼580 nm),[26] but quite different from those of the corresponding diamagnetic dimers ($[PQ_{rad}^-]_2$: $\lambda_{max}$ = 440 and 670 nm, [9-decarboxy-$PQQ_{rad}^-]_2$: $\lambda_{max}$ = 460 and ∼670 nm).[25,26] Thus, $\mathbf{1}_{rad}Me^-$ exists as a paramagnetic monomer in $CH_2Cl_2$. Bulk electrolysis of the resulting solution of $\mathbf{1}_{rad}Me^-$ at 0.0 V vs $Ag/Ag^+$ regenerated quinone $\mathbf{1}_{ox}Me$ quantitatively (Figure 4B), agreeing well with the reversibility observed in the cyclic voltammetric measurement (Figure 2A).

ESR spectra of the semiquinone radical anion species were measured by using the electrolysis cell designed for ESR measurements (see Experimental Section). Electrolysis on a helical gold wire with large surface area (12 $cm^2$) in the ESR quartz cell (5 mm diameter) can steadily generate the semiquinone radical anion species at a concentration high enough for the ESR measurements (∼$10^{-5}$ M), even though side reactions such as protonation or disproportionation occur.[17] Thus, we were able to detect well-resolved solution ESR spectra not only of $\mathbf{1}_{rad}Me^-$ but also of $\mathbf{1}_{rad}H^-$ as shown in Figure 5, panels a and b, respectively. Bulk electrolysis of $\mathbf{1}_{ox}Me$ or $\mathbf{1}_{ox}H$ (1 mM) in $CH_2Cl_2$ containing 0.1 M $NBu_4PF_6$ at −0.80 V vs

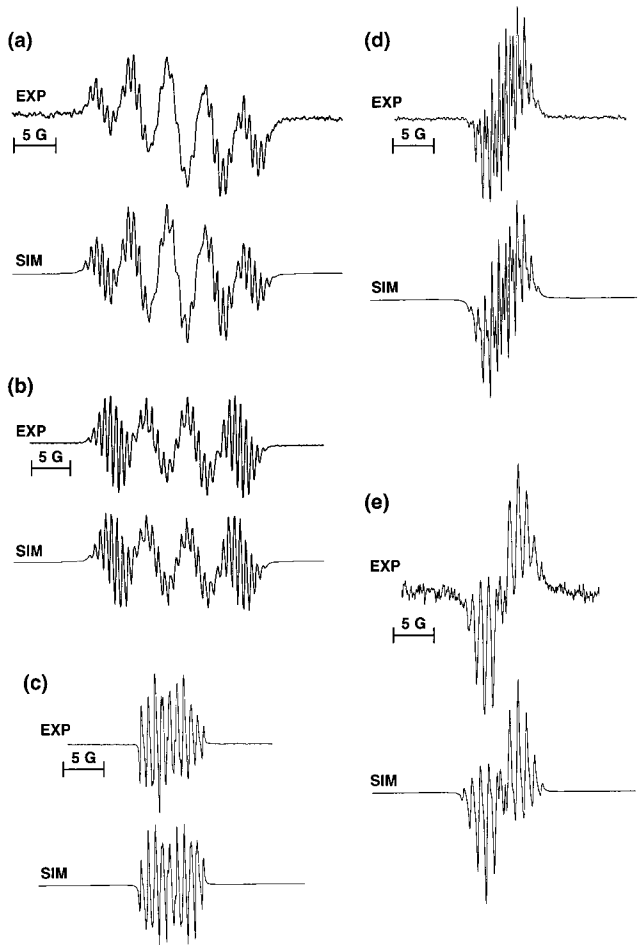


**Figure 5.** ESR spectra of (a) $\mathbf{1}_{rad}Me^-$ electrochemically generated at −0.8 V vs $Ag/Ag^+$ in $CH_2Cl_2$, (b) $\mathbf{1}_{rad}H^-$ electrochemically generated at −0.7 V vs $Ag/Ag^+$ in $CH_2Cl_2$, (c) $\mathbf{1}_{rad}^{2-}$ electrochemically generated at −1.0 V vs $Ag/Ag^+$ in MeCN, (d) $\mathbf{1}_{rad}Me^-$ electrochemically generated at −0.8 V vs $Ag/Ag^+$ in MeCN, and (e) $\mathbf{1}_{rad}Me^-$ electrochemically generated at −0.8 V vs $Ag/Ag^+$ in the presence of $Ca(ClO_4)_2$ (1 equiv 1.0 mM) in MeCN at 25 °C. Line widths of the simulations are (a) 0.27, (b) 0.30, (c) 0.15, (d) 0.25, and (e) 0.20 G, respectively.

$Ag/Ag^+$ in the ESR cavity gave a strong isotropic signal whose *g* value is within a range of ordinary semiquinone radical anion species ($\mathbf{1}_{rad}Me^-$, $g$ = 2.0034; $\mathbf{1}_{rad}H^-$, $g$ = 2.0041).[27] The hyperfine structures of the radical anion species are well reproduced by the computer simulation with the hyperfine splitting (hfs) values listed in Table 2 (Figure 5, SIM). On the basis of the calculated atomic orbital spin populations of the semiquinone radical anion species by the PM3 method (see

(25) Staples, T. L.; Szwarc, M. *J. Am. Chem. Soc.* **1970**, *92*, 5022.
(26) Rodriguez, E. J.; Bruice, T. C.; Edmondson, D. E. *J. Am. Chem. Soc*. **1987**, *109*, 532.
(27) (a) Swarz, H. M.; Bolton, J. R.; Borg, D. C. *Biological Applicaton of Electron Spin Resonance*; John Wiley & Sons: New York, 1972; p 24. (b) Fukuzumi, S.; Nishizawa, N.; Tanaka, T. *J. Org. Chem.* **1984**, *49*, 3571.

Supporting Information, Figures S3 and S4), the observed hyperfine splitting (hfs) values could be assigned as listed in Table 2, although assignment of the hfs values for methyl ester protons is ambiguous at present.[28]

Bulk electrolysis of $\mathbf{1}_{ox}$Me in MeCN containing 0.1 M $NBu_4PF_6$ at −0.8 V vs $Ag/Ag^+$ gave a different ESR spectrum (shown in Figure 5d that can be also simulated by the hfs values for two protons, one set of methyl protons, and two nitrogen atoms as listed in Table 2. The hfs values of $\mathbf{1}_{rad}Me^-$ in MeCN is significantly smaller than those obtained in $CH_2Cl_2$ except $a_{Me(1)}$, the reason for which is discussed below. Furthermore, bulk electrolysis of $\mathbf{1}_{ox}$H in MeCN at −1.0 V vs $Ag/Ag^+$ gave the ESR spectrum of $\mathbf{1}_{rad}^{2-}$ ($g = 2.0039$), which is generated by one-electron reduction of $\mathbf{1}_{ox}^-$ (eq 3) formed from $\mathbf{1}_{ox}$H via deprotonation by electrochemically generated $\mathbf{1}_{rad}H^-$ in situ (eq 4). The ESR spectrum of $\mathbf{1}_{rad}^{2-}$ in MeCN shown in Figure 5c is essentially the same as that of $\mathbf{1}_{rad}^{2-}$ generated by bulk electrolysis of $\mathbf{1}_{ox}^-K^+$ in DMSO containing 0.1 M $NBu_4PF_6$ at −1.0 V vs $Ag/Ag^+$. The ESR spectrum can be reproduced perfectly by the computer simulation using hfs values of just two protons and two nitrogen atoms, confirming the deprotonation of the pyrrole proton (1-NH). On the basis of the molecular orbital calculation (see Supporting Information, Figure S5), we assigned the hfs value as $a_{H(3)} = 0.87$ G, $a_{H(8)} = 3.51$ G, $a_{N(1)} = 0.90$ G, and $a_{N(6)} = 0.70$ G as listed in Table 2. Deprotonation of $\mathbf{1}_{rad}H^-$ to give $\mathbf{1}_{rad}^{2-}$ resulted in a significant change of the spin distribution. In $\mathbf{1}_{rad}H^-$ and $\mathbf{1}_{rad}Me^-$, the spin density on the pyrrole ring is higher than that on the pyridine nucleus, but the spin density on the pyrrole ring becomes significantly small in $\mathbf{1}_{rad}^{2-}$.

Solvent effects on the electronic structures of the semiquinone radical anion species are evident. Kano et al. reported a well-resolved solution ESR spectrum of electrochemically generated radical anion of native PQQ taken in an alkaline aqueous solution at pH 12.[11b] They determined the hfs values as 0.60 and 0.81 G for two nitrogens and as 0.94, 1.24, and 1.84 G for hydrogens by computer simulation. Bruice et al. also reported the hfs values of the radical anion species of 9-decarboxy-PQQ in $Na_2CO_3$ buffer at pH 10.47 as 0.60 and 0.81 G for two nitrogens and as 1.02 (NH-1), 1.26, 0.80 (H-9), and 1.84 G for hydrogens.[26] Judging from the large difference of the hfs values between $\mathbf{1}_{rad}H^-$ or $\mathbf{1}_{rad}Me^-$ in the less polar organic solvent ($CH_2Cl_2$) and the radical anion species of PQQ or 9-decarboxy-PQQ in alkaline aqueous solutions, the spin density is much more delocalized in the former cases than in the latter cases. In other words, effective solvation by water molecule leads to localization of the negative charge and the spin onto the quinone moiety of the PQQ molecule in the case of PQQ and 9-decarboxy-PQQ in alkaline aqueous solutions. Thus, themodynamic stability of the semiquinone radical anion is much enhanced in alkaline aqueous solutions than in nonpolar organic media because of the strong solvation by water molecules. In fact, the one-electron redox potential of $PQQ/PQQ_{rad}^-$ in water (−0.33 V vs SCE)[11b] is significantly less negative than that of $\mathbf{1}_{ox}Me/\mathbf{1}_{rad}Me^-$ (−0.53 vs SCE)[29] in $CH_2Cl_2$. The smaller hfs values of $\mathbf{1}_{rad}Me^-$ in MeCN than those in the less polar solvent $CH_2Cl_2$ (Table 2) may also be attributed to the effective solvation by MeCN leading to localization of the negative charge and the spin onto the quinone moiety.

(28) The $a_{N(1)}$ and $a_{N(6)}$ can be readily distinguished because of the much larger spin density at N(1) than N(6). The $a_{H(3)}$ and $a_{H(8)}$ can also be assigned based on the significantly larger spin density on C(3) than C(8) (see Supporting Information, Figures S3−S5).

(29) The redox potentials measured vs ferrocene/ferrocenium are converted to those vs SCE by adding 0.37 V.

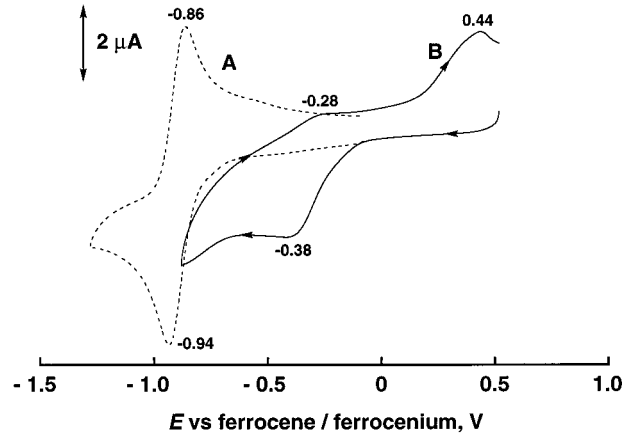


**Figure 6.** Cyclic voltammograms of $\mathbf{1}_{ox}$Me (1.1 mM) (A) in the absence of $Ca(ClO_4)_2$ and (B) in the presence of $Ca(ClO_4)_2$ (1.1 mM) in deaerated MeCN at 298 K.

**Effects of Calcium Ion on the One-Electron Reduction of $\mathbf{1}_{ox}$Me.** Addition of an equimolar amount of $Ca(ClO_4)_2 \cdot nH_2O$ into an MeCN solution of $\mathbf{1}_{ox}$Me resulted in as large as 0.57 V positive shift of the one-electron redox potential of the quinone, although corresponding oxidation peak (at −0.28 V) became smaller due to the protonation of the generated semiquinone radical anion species by hydrated water (Figure 6B). In fact, an irreversible anodic peak for the oxidation of the $Ca^{2+}$ complex of $\mathbf{1}_{red}MeH_2$ appeared at 0.44 V vs $Fc/Fc^+$ as in the case of $\mathbf{1}_{ox}$Me plus acetic acid (see Figure 2). $\mathbf{1}_{red}MeH_2$ is generated by protonation of $\mathbf{1}_{rad}Me^-$ with the hydrated water of $Ca(ClO_4)_2 \cdot nH_2O$ and the disproportionation of resulting $\mathbf{1}_{rad}$-MeH (similar to eqs 4 and 6). Thus, it can be concluded that the oxidation power of PQQ in MDH is enhanced significantly by the $Ca^{2+}$ coordination as compared to free PQQ.

The well-resolved solution ESR spectrum of the $Ca^{2+}$ complex of $\mathbf{1}_{rad}Me^-$ in MeCN can be obtained successfully by using the electrolysis cell with the helical gold wire with large surface area as shown in Figure 5e. The ESR spectrum can be reproduced perfectly by the computer simulation using hfs values in which the $a_{N(6)}$ value becomes larger by the complexation with $Ca^{2+}$ while the other hfs values are not perturbed significantly. This indicates that $Ca^{2+}$ binds to the pyridine nitrogen as in the case of the $Ca^{2+}$ complex of $\mathbf{1}_{ox}$H.[10b,c] Molecular orbital calculations also suggest that type A binding mode is much more stable than type B binding mode by ca. 33 kcal $mol^{-1}$ (type A: $H_f = -191.318$ kcal $mol^{-1}$, type B: $H_f = -158.102$ kcal $mol^{-1}$, calculated by the PM3 method using Spartan Version 5.0).

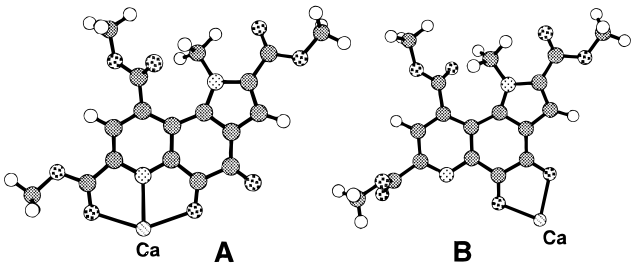


**Summary.** Details about the electrochemical behavior and electronic structures of semiquinone radical anion species of coenzyme PQQ in aprotic organic media have been explored by means of cyclic voltammetry (CV), ESR, and thin-layer UV−vis techniques. It has been found that the existence of the active pyrrole proton of PQQ causes the complexity of the electro-

chemistry of the trimethyl ester of coenzyme PQQ in aprotic organic media. Nonetheless, the one-electron reduction potential of the trimethyl ester of PQQ ($\mathbf{1}_{ox}$H) has been determined as ca. −0.9 V vs $Fc/Fc^+$ in $CH_2Cl_2$. This value is ca. 0.4 V higher than the one-electron reduction potential of flavin coenzyme under the same conditions. The ESR studies on the electrochemically generated semiquinone radical anion species clearly indicate that the spin distribution of the radical anion is significantly altered by the solvents. This can be attributed to the difference of solvation effect; the polar solvent (MeCN) effectively solvates the radical anion species at the quinone moiety, where the spin becomes more localized, whereas the spin is delocalized into the whole molecule in the nonpolar solvent ($CH_2Cl_2$). The complex formation with $Ca^{2+}$, which is another cofactor of quinoprotein alcohol dehydrogenase, resulted in ca. 0.57 V positive shift of the one-electron reduction potential of the quinone. The ESR spectrum of $Ca^{2+}$ complex of the semiquinone radial anion has been compared with that of the free semiquinone radical anion to explore the binding position of $Ca^{2+}$. The information about the electrochemistry of coenzyme PQQ and the characterization of the semiquinone radical anion species of PQQ in aprotic solvents will provide valuable insight into the redox function of coenzyme PQQ in several living systems.

**Acknowledgment.** The present study was financially supported in part by a Grant-in-Aid for Scientific Research on Priority Area (Molecular Biometallics: 10129218; Electrochemistry of Ordered Interface: 10131242; Creation of Delocalized Conjugated Electronic Systems: 10146232) and a Grant-in-Aid for General Scientific Research (08458177) from the Ministry of Education, Science, Sports, and Culture of Japan. Our special thanks are due to Professor K. Tajima of Kyoto Institute of Technology for supplying the electrolysis cell designed for the ESR measurements.

**Supporting Information Available:** Comparison of the cyclic voltammograms of $\mathbf{1}_{ox}$H and $\mathbf{1}_{ox}$Me in deaerated $CH_2Cl_2$ (S1), the thin-layer UV−vis spectrum of a bulk electrolysis solution ($CH_2Cl_2$) of $\mathbf{1}_{ox}$H and the computer-generated spectrum (S2), and calculated spin density maps of $\mathbf{1}_{rad}H^-$ (S3), $\mathbf{1}_{rad}Me^-$ (S4), and $\mathbf{1}_{rad}^{2-}$ (S5) (5 pages, print/PDF). See any current masthead page for ordering information and Web access instructions.

JA9813663